Phase transitions induced by proton tunneling in hydrogen-bonded crystals. Ground-state theory

Kenneth S. Schweizer and Frank H. Stillinger
AT&T Bell Laboratories, Murray Hill, New Jersey 07974
(Received 12 August 1983)

A novel theory is presented for the ground-state equilibrium properties and phase behavior of hydrogen-bonded crystals in which quantum-mechanical tunneling is important. The approach is based on a variational correlated wave function and simultaneously treats short- and long-range proton correlations in addition to the quantum tunneling aspect. Application to an exactly solvable quantum spin model along with general statistical mechanical considerations suggest the theory is quantitatively reliable for many three-dimensional crystals of interest. Model calculations reveal a diverse set of possible phase behaviors as a function of applied pressure. The theory should be useful for predicting and interpreting a range of phenomena induced by high pressure (e.g., order-disorder phase transitions, dielectric properties, hydrogen-bond symmetrization) for experimentally interesting systems such as the KDP-like (potassium dihydrogen phosphate) ferroelectrics and ice polymorphs.

I. INTRODUCTION

Many crystalline materials contain pairs of oxygen atoms connected by hydrogen bonds. By lowering the temperature, some of these substances undergo order-disorder phase transformations to states of spontaneously broken symmetry characterized by long-range proton order. In addition, these materials display strong short-range correlations between the interacting protons both above and below the transition temperature. The ferroelectric potassium dihydrogen phosphate (KDP) and the antiferroelectric ice VIII polymorph are classic examples of such hydrogen-bonded crystals. In the latter case, the short-range order at ordinary pressures gives rise to a structure comprised almost exclusively of intact water molecules that are hydrogen-bonded according to the so-called Bernal-Fowler-Pauling ice rules.[1] Indeed, for most hydrogen-bonded crystals at low pressures the position of the bridging hydrogen is found (as in the ice example) to be well off the bond midpoint, and hence can be taken to "belong" to one of the participating oxygens.

A distinguishing feature of hydrogen-bonded materials is the possibility of quantum-mechanical tunneling of the proton between the two equivalent minima along the bond connecting the two oxygens. For most systems at ordinary pressures the corresponding tunnel splitting is either negligible or rather small ($\lesssim 50$ cm^{-1}), and thus the consequences of such a process are modest. The phase behavior of crystals under these conditions has been extensively investigated both experimentally and theoretically.[2]

Modification of the above picture is expected to occur upon reduction of the oxygen-oxygen separation via application of external pressure. Structural studies have revealed[3,4] the general correlation that the covalent O—H bond lengths stretch as R_{OO}, the distance between hydrogen-bonded oxygens, decreases. This behavior leads to a significant reduction of the potential barrier separating the two equivalent minima and hence to an increase of quantum fluctuations via tunneling. Under these circumstances, a range of fascinating phenomena can be envisioned. A partial list includes the possible destruction of the long-range proton-ordered state by quantum fluctuations, abnormally large concentrations of ionic configurations, and symmetrization of the hydrogen bond.[5] Even the concept of a crystal such as ice being composed of intact water molecules may begin to break down in favor of an ionic or covalent solid picture. These questions are of particular interest in the low-temperature regime where the system is strongly ordered at ordinary pressures and the consequences of quantum tunneling are not obscured by thermal fluctuations.

Unfortunately, previous theoretical work is inadequate for a realistic description of such highly quantum-mechanical phenomena. In particular, simple mean-field theory (MFT) considers only the long-range-order aspect, thereby neglecting all short-range proton correlations and predicting second-order phase transitions. Attempts to go beyond this description by including the strong short-range proton order consist of truncated cluster expansions about a mean-field reference system.[6–8] These theories are inherently high-temperature approximations which are valid only when the energy scale characterizing the quantum fluctuations is small, or at most of the order of the thermal energy. They possess the catastrophic feature of exhibiting an anti-Curie point at low temperatures.[6] Consequently, a reliable theory beyond MFT for a strongly quantum system that includes detailed short-range correlations does not seem to exist.

The purpose of the present paper is to develop an accurate theory that addresses the questions of short-range order, long-range order, and strong quantum fluctuations. As shown elsewhere,[9] for many systems the tunneling-driven phase transitions occur at sufficiently high pressure that in the low-temperature regime [$T \lesssim \frac{1}{2} T_c$ (1 atm)] the thermal fluctuations are expected to play a minor role. Consequently, we consider here only the zero-temperature

 ©1984 The American Physical Society

quantum ground-state problem. Our formulation is sufficiently general to allow treatment of a wide range of hydrogen-bonded ferroelectrics and also ice polymorphs. Applications to specific materials, including the questions of high ion concentrations and hydrogen-bond symmetrization, will be reserved for future work.[9,10] Here we concentrate on the general consequences of strong quantum fluctuations in hydrogen-bonded ferroelectrics.

The remainder of the paper is structured as follows. The basic Hamiltonian model will be discussed in Sec. II and material-specific features will be identified. A correlated wave-function theory for this model is developed in Sec. III. Section IV compares the predictions of this theory with known results for an exactly solvable problem, the one-dimensional transverse Ising model. The predictions and general characteristic features of the theory for the full three-dimensional ferroelectric case are explored in Sec. V via model calculations. The paper concludes with a discussion of the applicability and significance of this work, along with future directions of research.

II. MODEL

The Hamiltonian model we consider is very similar to that applied by previous workers to the hydrogen-bonded ferroelectric problem.[6,11–13] We shall therefore be brief in our description and concentrate on developing a notation relevant to our subsequent variational ground-state theory.

We begin by invoking the simplifying assumption that the lattice (e.g., oxygens for ice, phosphate groups and potassium ions for KDP) is static. Attention is therefore focused entirely on the protonic motions and interactions. For the purpose of calculating the proton-proton potential energy we adopt a two-state description where each proton is localized on one or the other side of the bond corresponding (at low pressure) to positions of potential minima. The configuration of the jth proton is therefore mathematically described by the z-component Pauli spin operator S_j^z, which can take on the values ± 1. For the hydrogen-bonded crystals of interest, we define a "vertex" as the elementary four-coordinated objects which are connected via the hydrogen bonds. For example, in ice the oxygen atoms are the vertices while for KDP the corresponding objects are the phosphate (PO_4) groups. Each vertex can be classified by the configuration ("near" or "far") of the four protons surrounding it. Such a classification can be based on merely the ionic character (i.e., the number of protons that belong to a vertex) or possibly on a more detailed scheme.

For a realistic description of the short-range interactions between the four protons around a given vertex, it is necessary to distinguish the changes in local potential energy associated with each distinct vertex state (e.g., OH^-,H_2O,H_4O^{2+} for ice). This requires the introduction of four-proton interactions in a potential energy of the form

$$U=\sum_{\nu}\sum_{(i,j,k,l)\in\nu} I_{ijkl}S_i^zS_j^zS_k^zS_l^z+\sum_{i>j}{}' J_{ij}S_i^zS_j^z\ . \tag{2.1}$$

The first term in Eq. (2.1) describes the short-range coupling between the four protons around a vertex ν. A specific proton configuration (i,j,k,l) is assigned the energy I_{ijkl}. The second term represents a two-body residual coupling between protons that describes the longer-range interaction (typically dipolar) between more distance protons. Even in the absence of quantum effects, the statistical mechanics of such a model is too difficult to allow rigorous treatment. We follow the common approach and replace this potential-energy function by a simpler one

$$\begin{aligned} V&=\sum_{\alpha}\epsilon_\alpha N_\alpha+NJ(1-2x)^2 \\ &\equiv V_{\rm SR}+V_{\rm LR}\ . \end{aligned} \tag{2.2}$$

Here $V_{\rm SR}$ represents the energies associated with creation of a vertex of type α and N_α is the number of such vertices. As such, it describes the short-range order of protons around a given vertex in the extreme shielding limit. The second term, $V_{\rm LR}$, treats the longer-range residual interactions in an effective or mean-field fashion. It explicitly defines a proton configuration of lowest long-range potential energy, $-2NJ$ (where $2N$ is the number of protons in the crystal), and introduces the long-range-order parameter, x $(0\le x\le 1)$, that denotes the fraction of protons in the "wrong" positions as defined by the uniquely specified state $x=0$. (Note that there is a symmetry about $x=\frac{1}{2}$ which simply reflects the fact that the configurations corresponding to all protons in the "right" position and all protons in the wrong position are equivalent energetically.) For ferroelectric materials, $1-2x$ is often proportional to the macroscopic spontaneous polarization; for antiferroelectrics it can be identified with the sublattice or staggered polarization. Its specific meaning will depend on the nature of the ordered state of the crystal of interest. The physical meaning of the second term in Eq. (2.2) lies in the realization that for any real system different proton configurations with the same number of vertex types (short-range order) are not energetically degenerate. For example, in ice there are approximately $(\frac{3}{2})^N$ (where N is the number of oxygen atoms) neutral water molecule configurations which are very close in energy but not exactly degenerate. The second term provides a mechanism for the lifting of this degeneracy in a simple mean-field fashion.

An important feature of the form of the model potential energy of Eq. (2.2) is its dependence on microscopic vertex types and their numbers $\{N_\alpha,Nx\}$. These number operators describe the short- and long-range proton order, respectively, and their introduction anticipates the order-parameter nature of any theory based on Eq. (2.2). As a technical point, we note in passing that Eq. (2.2) can be written explicitly in terms of the real-space proton positions by employing the Pauli spin operators, S_i^z, and introducing the appropriate fermion projection operators.[6] However, for our subsequent purposes this transcription is not necessary.

Modest quantum effects due to the small proton mass have been directly observed in many hydrogen-bonded ferroelectric crystals by performing isotope substitution studies. In addition, under pressure the character of the bistable potential that a proton moves in along the bond can be significantly altered. As previously mentioned the

separation between the two equivalent minima and the barrier separating them can be greatly reduced. This leads to an enhancement of the resonance splitting of the proton ground vibrational state and a more rapid tunneling of the proton from one side of the bond to the other. We make the simplifying approximation of retaining only these lowest two resonance-split quantum states. Diagonalization of the single-particle Schrödinger equation yields the two lowest eigenstates, $\Phi_0(r)$ and $\Phi_1(r)$, and the corresponding energies E_0,E_1. By constructing the symmetric and antisymmetric linear combinations of these eigenstates one obtains states that are localized primarily on one side of the bond. These latter states represent the analog of the localized classical two-state proton description and correspond to $S_l^z=\pm 1$. Such a construction is meaningful even when the intervening barrier between the two-potential minima is small, or even nonexistent.[5] The energy difference between the two lowest single-proton states is characterized by a tunnel splitting parameter, K, defined to be $2K\equiv E_1-E_0$, and is a measure of the size of quantum fluctuations. In terms of the two-state model the quantized proton motion contributes a one-body kinetic energy term of the form

$$T\equiv -K\sum_{l=1}^{2N} S_l^x \,, \tag{2.3}$$

where S_l^x has its standard Pauli spin operator meaning. The complete model Hamiltonian we shall consider is given by the combination of Eqs. (2.2) and (2.3).

We note that the present model is nearly identical to that adopted by Blinc and Svetina in their study of KDP-like ferroelectrics.[6] The specific properties of a particular material enter the theory via the energies ϵ_α, J, and K. In general, these will be pressure dependent to varying degrees. Modifications of the model to include other types of interactions such as short-range ion-ion coupling or two-body tunneling effects can be appended if desired, but for the sake of simplicity will not be pursued here. Finally, we observe that the present model does not depend explicitly on the entire lattice topology but only on the four-fold coordination of the vertices.

III. THEORY

As discussed in Sec. II, the potential energy we have adopted is entirely specified by the numbers, $\{N_\alpha\}$, and energies, $\{\epsilon_\alpha\}$, of the vertex charge states and the fraction of protons in the wrong position, x. Therefore, a full classification of the vertices is defined by how many, and what types [right (r) or wrong (w)] of protons are attached. An example of such a classification scheme for a tagged vertex is shown in Fig. 1. Within this framework, the $2^4=16$ possible proton configurations around a particular vertex can be grouped into nine distinct vertex types and their corresponding numbers: N_{rrww},N_{rrw},N_{rww}, $N_{rr},N_{rw},N_{ww},N_r,N_w,N_0$. The subscripts in the present notation refer to the protons that are near (belong to) the tagged vertex. For the systems of interest to us, the vertex carries a formal charge q. For the case of ice, $q=-2e$ for the oxygen atom vertex. Therefore, since the proton is singly charged, the ionicity of the above nine possible states are $(+2,+1,+1,0,0,0,-1,-1,-2)e$, respectively.

The explicit form of the model potential energy is

$$V=\epsilon_1(N_{rrw}+N_{rww}+N_r+N_w)+\epsilon_2(N_{rrww}+N_0) -\lambda(N_{rr}+N_{ww})-2NJ(1-2x)^2 \,. \tag{3.1}$$

The following four characteristic energies have been introduced.

(1) The energy of a singly charged ion, ϵ_1 [assumed to be the same for the cation (three protons near the vertex) and anion (one proton near the vertex)].

(2) The energy of a doubly charged ion, ϵ_2.

(3) The stabilization energy per vertex, $-\lambda$, of the two neutral states (N_{rr},N_{ww}) relative to the other four neutral configurations. For a perfect tetrahedral arrangement of hydrogen bonds around a vertex we expect $\lambda=0$. However, for many materials (e.g., KDP) there exists a preferred crystal axis which lifts the degeneracy of the six neutral configurations. The parameter λ accounts for such configurational anisotropy.

(4) The long-range protonic interaction (generally dipolar) energy, J, that contributes to the stabilization of the lowest energy classical ground state.

Five of the ten variables $(\{N_\alpha\},x)$ of the above description can be eliminated by employing the following relations: For the vertex number conservation

$$N_{rrww}+N_{rrw}+N_{rww}+N_{rr}+N_{rw}+N_{ww}+N_r +N_w+N_0=N \,, \tag{3.2}$$

where N is the number of vertices. For charge neutrality

$$2N_{rrww}+N_{rrw}+N_{rww}-N_r-N_w-2N_0=0 \,. \tag{3.3}$$

For long-range-order definition

$$2(N_{rrww}+N_{rww}+N_{ww})+N_{rrw}+N_{rw}+N_w=2Nx \,. \tag{3.4}$$

Charge conjugation symmetry leads to the expectation that to within negligible fluctuations of order $N^{-1/2}$

$$N_{rrww}=N_0,\quad N_{rrw}=N_r,\quad N_{rww}=N_w \,. \tag{3.5}$$

Utilization of the above relations allows a description in terms of five independent variables which we choose to be $N_{rr},N_{ww},N_{rw},N_0,x$. In terms of this set, the potential ener-

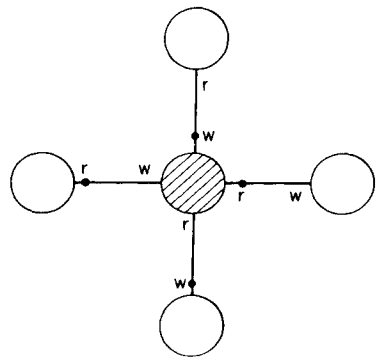

FIG. 1. Four-coordinated vertex with the two possible proton positions along each bond labeled as right (r) or wrong (w). The above proton configuration corresponds to a neutral vertex that is a member of the N_{rw} type.

gy per proton is given by

$$V/2N=\epsilon_1(x_r+x_w)+\epsilon_2 x_0-\lambda(x_{rr}+x_{ww})/2 -J(1-2x)^2 , \tag{3.6}$$

where the vertex-type concentrations, $x_\alpha \equiv N_\alpha/N$, have been introduced and

$$x_r \equiv x-\tfrac{1}{2}+\tfrac{1}{4}(x_{rr}-x_{rw}-3x_{ww}-2x_0) , \tag{3.7}$$

$$x_w \equiv \tfrac{3}{4}-x+\tfrac{1}{4}(x_{ww}-x_{rw}-3x_{rr}-2x_0) . \tag{3.8}$$

For the purely classical problem the adoption of a potential energy that depends only on the number of vertex types implies a degeneracy or entropy associated with the number of distinct proton configurations, $\Omega(\{N_\alpha\},x)$, that yield the same vertex type numbers $\{N_\alpha,x\}$. Assuming a random arrangement of vertex types subject only to the global constraints specified by a fixed $\{N_\alpha,x\}$, one obtains an explicit expression for the degeneracy factor,

$$\begin{aligned}\Omega(\{N_\alpha\},x)&=\frac{N!}{N_{rrww}!N_0!N_r!N_w!N_{rr}!N_{rw}!N_{ww}!N_{rrw}!N_{rww}!} \\ &\times\left(\tfrac{1}{16}\right)^{N_{rrww}+N_{rr}+N_{ww}+N_0}\left(\tfrac{2}{16}\right)^{N_{rrw}+N_{rww}+N_r+N_w}\left(\tfrac{4}{16}\right)^{N_{rw}}x^{2Nx}(1-x)^{2N(1-x)} \\ &=\frac{N!2^{N+N_{rw}-N_{rr}-N_{ww}-2N_0}}{(N_0!)^2(N_r!)^2(N_w!)^2N_{rr}!N_{ww}!N_{rw}!}x^{2Nx}(1-x)^{2N(1-x)} .\end{aligned} \tag{3.9}$$

In the first line of Eq. (3.9), the leading factor is the appropriate multinomial coefficient, followed by the set of local attrition factors (probabilities), and the last factor arises from the single-proton long-range-order probability. This form is directly analogous to that employed by Slater[11] and Takagi[12] for their slightly more restrictive models. We note in passing that upon combining Eqs. (3.6)—(3.9) one obtains the Slater-Takagi-Senko classical theory for the partition function

$$Z_{\text{class}}=\sum_{\{N_\alpha,x\}}\Omega(\{N_\alpha\},x)e^{-\beta V[\{N_\alpha\},x]} . \tag{3.10}$$

We now turn to the inclusion of quantum tunneling. A completely general form for the ground-state wave function can be written as a linear combination of the orthonormal Hartree orbitals

$$\Psi=\sum_{\{S_k^z\}}A(\{S_k^z\})\prod_{j=1}^{2N}\Phi_j(S_j^z;\{S_k^z\}) , \tag{3.11}$$

where $\{S_k^z\}$ denotes a particular configuration (out of the 2^{2N} possibilities) of all the protons and $\Phi_j(S_j^z;\{S_k^z\})$ specifies which side of the bond proton j is on for the configuration $\{S_k^z\}$. From Eq. (3.11), it is obvious that $|A(\{S_k^z\})|^2$ is the probability the system can be found in the configuration $\{S_k^z\}$. To make further progress, we must invoke a simplification that removes the dependence of the many-body wave-function amplitudes on the specific $\{S_k^z\}$ configuration. The form of the model potential energy [Eq. (3.6)] is suggestive in this regard. Since it depends on the specific proton configuration only through the total number of vertex state types and long-range-order parameter, all $\{S_k^z\}$ corresponding to the same set of order parameters are equally probable in the classical theory. The natural extension of this feature to the quantum-mechanical situation is to assume a trial wave function of the form

$$\begin{aligned}\Psi_t&\equiv\sum_{\{S_k^z\}}A(\{N_\alpha(\{S_k^z\}),x\})\prod_{j=1}^{2N}\Phi_j(S_j^z;\{S_k^z\}) \\ &=\sum_{\{N_\alpha,x\}}A(\{N_\alpha\},x)\sum_{\{S_k^z\}\in\{N_\alpha,x\}}\prod_{j=1}^{2N}\Phi_j(S_j^z;\{S_k^z\}) .\end{aligned} \tag{3.12}$$

We shall refer to this form as a "random-mixing" approximation since it requires all proton configurations corresponding to a fixed set $\{N_\alpha,x\}$ to be equally probable. For a fixed set of $\{N_\alpha,x\}$ the real space proton positions are *random* subject only to the global vertex number constraints and geometrical constraints such as the impossibility of having two nearest-neighbor vertices both in the doubly charged cation state. Normalization of the trial wave function requires

$$\sum_{\{N_\alpha,x\}}A^*(\{N_\alpha,x\})A(\{N_\alpha,x\})\Omega(\{N_\alpha,x\})=1 . \tag{3.13}$$

We proceed by calculating the trial energy

$$\begin{aligned}E&\equiv\langle\Psi_t|H|\Psi_t\rangle \\ &=\langle\Psi_t|V|\Psi_t\rangle+\langle\Psi_t|T|\Psi_t\rangle .\end{aligned} \tag{3.14}$$

The potential-energy matrix element is easily computed since by construction the potential-energy operator is diagonal in the representation of the trial wave function

$$\begin{aligned}\langle\Psi_t|V|\Psi_t\rangle&=\sum_{\{N_\alpha,x\}}V(\{N_\alpha\},x)\Omega(\{N_\alpha,x\})A^2(\{N_\alpha,x\}) \\ &=V(\{\bar{N}_\alpha,\bar{x}\}) .\end{aligned} \tag{3.15}$$

In the second line of the above equation, $\{\bar{N}_\alpha,\bar{x}\}$ represents the (ground-state) average values of the order parameters. This reduction is valid since fluctuations in the order parameters are $O(1/N)$ and hence vanish in the large-system-size limit.

Employing Eq. (2.3) the kinetic energy (tunneling) matrix element is given by

$$\langle \Psi_t \mid T \mid \Psi_t \rangle = \left\langle \Psi_t \left| \left[-K \sum_{l=1}^{2N} S_l^x \right] \right| \Psi_t \right\rangle$$
$$= -2NK \langle \Psi_t \mid S_1^x \mid \Psi_t \rangle$$
$$\equiv -2NKS \, . \tag{3.16}$$

The operator S_1^x induces proton jumps in a single tagged bond and hence can give rise to changes in the $\{N_\alpha,Nx\}$, only in increments of 0, ± 1, or ± 2. Employing Eq. (3.12) we have

$$S = \sum_{\{N_\alpha,x\}} \sum_{\{N'_\alpha,x'\}} \Omega(\{N_\alpha,x\}) A^*(\{N_\alpha,x\}) A(\{N'_\alpha,x'\})$$
$$\times \left[\Omega^{-1}(\{N_\alpha,x\}) \sum_{\{S_k^z\} \in \{N_\alpha,x\}} \sum_{\{S_k'^z\} \in \{N'_\alpha,x'\}} \langle \Phi_1(\{N_\alpha,x\}) \mid S_1^x \mid \Phi_1(\{N'_\alpha,x'\}) \rangle \right] \prod_{j(\neq 1)}^{2N} \delta_{S_j^z,S_j^z} \, . \tag{3.17}$$

For any particular configuration $\{S_j^z\} \in \{N_\alpha,x\}$ in the sum in Eq. (3.17), the matrix element is nonzero only for a uniquely specified single configuration $\{S_k'^z\}$. In addition, for a specific $\{N_\alpha,x\}$, the probability that the two connected vertices associated with the tagged proton 1 are a particular type is determined by the random-mixing statistics. This allows one to write

$$S = \sum_{\{N_\alpha,x\}} \Omega(\{N_\alpha,x\}) A^*(\{N_\alpha,x\})$$
$$\times \left[\sum_{\{N'_\alpha,x'\}} A(\{N'_\alpha,x'\}) T(\{N_\alpha,x\} \mid \{N'_\alpha,x'\}) \right] , \tag{3.18}$$

where $T(\{N_\alpha,x\} \mid \{N'_\alpha,x'\})$ is the probability that two system configurations selected at random from the $\{N_\alpha,x\}$ and $\{N'_\alpha,x'\}$ sets differ only at bond number 1. To calculate these probabilities we first observe that the "state" of a bond is defined by (a) which side the proton is on, and (b) the states of the two vertices connected by the bond. For a particular bond, the two attached vertices are distinguished as either proton (p) or hole (h) depending on whether the proton belongs or does not belong to the vertex, respectively. One then proceeds to compute the fraction of the $\Omega(\{N_\alpha,x\})$ configurations which have the two ends of the tagged polarized bond specified by a particular pair of vertex types. This fraction is given by a product of factors for the p and h ends of the polarized bond. For the model under consideration there are $2\times 6\times 6=72$ possible states that the tagged bond can initially have. When the proton tunnels to the other side (via the S_1^x operator) each of these is uniquely mapped into one of the other possible states. The 72 possibilities exist in pairs, differing only according to the end of the bond at which the proton initially resides. By accounting for all the possible "initial" states of the tagged bond, along with the appropriate probabilities for these states, one can evaluate the quantity in large parentheses in Eq. (3.18). We do not reproduce the algebraically complicated details here but refer the reader to Appendix A for a detailed treatment of an algebraically simpler case. An alternative, but equivalent, approach is discussed in Appendix B. Straightforward, but tedious, application of these methods to the present general case of interest yields a result of the form

$$S = \sum_{\{N_\alpha,x\}} \Omega(\{N_\alpha,x\}) A^*(\{N_\alpha,x\}) \sum_{k=r,w} \sum_{\sigma,\gamma} p^{(k)}(\sigma \mid \gamma;\{N_\alpha,x\}) A[f_{\sigma\gamma}(\{N_\alpha,x\})] \, , \tag{3.19}$$

where $p^{(r)}(\sigma \mid \gamma;\{N_\alpha,x\})$ $[p^{(w)}(\sigma \mid \gamma;\{N_\alpha,x\})]$ is the probability for the initial vertex number state $\{N_\alpha,x\}$ that the tagged bond connects vertices of type σ and γ with the proton in the right (wrong) position, and $\{N'_\alpha,x'\} \equiv f_{\sigma\gamma}(\{N_\alpha,x\})$ is the unique set of vertex-type numbers that result from transferring the proton from its initial side of the bond to the opposite one.

Combining Eqs. (3.14)–(3.16) and (3.19), one can derive an explicit expression for the trial energy. It is a functional of the wave-function amplitudes $A(\{N_\alpha,x\})$. Since the trial wave function is of the linear variational form, one can in principle functionally differentiate the trial energy (subject to the normalization constraint) with respect to the amplitudes and obtain equations for the entire eigenvalue spectrum. However, such a program generates functional equations that are in general intractable. We therefore concentrate on variationally determining only the ground-state energy. For this case the shifted argument amplitudes, $A[f_{\sigma\gamma}(\{N_\alpha,x\})] \equiv A(\{N_\alpha + n_\alpha^{\sigma\gamma}\})$, can be evaluated by noting that the probability for finding the system in a state characterized by $\{N_\alpha,x\}$ is

$$P(\{N_\alpha,Nx\}) \equiv \Omega(\{N_\alpha,Nx\}) A^2(\{N_\alpha,Nx\}) \, . \tag{3.20}$$

Since the $n_\alpha^{\sigma\gamma}$ numbers are of order one (specifically 0, ± 1, or ± 2), we have

$$P(\{N_\alpha + n_\alpha^{\sigma\gamma}\}) = P(\{N_\alpha\})[1 + O(1/N)] \, . \tag{3.21}$$

Therefore, in the thermodynamic limit ($N \to \infty$) one obtains

$$A(\{N_\alpha + n_\alpha^{\sigma\gamma}\}) = A(\{N_\alpha\})$$
$$\times [\Omega(\{N_\alpha\}) / \Omega(\{N_\alpha + n_\alpha^{\sigma\gamma}\})]^{1/2} . \tag{3.22}$$

Substitution of Eq. (3.22) in Eq. (3.19) yields

$$S=\sum_{\{N_\alpha,x\}}\left[\sum_{k=r,w}\sum_{\sigma,\gamma}p^{(k)}(\sigma\,|\,\gamma;\{N_\alpha,x\})\times[\Omega(\{N_\alpha\})/\Omega(\{N_\alpha+n_\alpha^{\sigma\gamma}\})]^{1/2}\right]\times\Omega(\{N_\alpha,x\})A^2(\{N_\alpha,x\})\,. \tag{3.23}$$

This expression is now of the same form as the diagonal potential energy matrix element [Eq. (3.15)]. Therefore, we can perform the summation in Eq. (3.23) to within corrections $O(1/N)$ by simply replacing the $\{N_\alpha,x\}$ by the average values $\{\bar{N}_\alpha,x\}$ as before. The result is a closed-form expression for the ground-state energy in terms of the (to be determined) average concentration parameters, $\{\bar{x}_\alpha\}$. These quantities are then treated as variational parameters determined via energy minimization

$$\frac{\partial F}{\partial\bar{x}_\alpha}\equiv 0\,. \tag{3.24}$$

Detailed calculation following the analysis outlined in Appendix A yields a trial ground-state energy per proton given by

$$E/2NK\equiv T/2NK+V/2NK\,, \tag{3.25}$$

$$\begin{aligned}T/2NK\equiv[x(1-x)]^{-1/2}\{&2x_0(x_rx_w)^{1/2}+x_0(x_r+x_w)+2x_{rw}(x_rx_w)^{1/2}\\&+x_r[2(x_0x_{rw})^{1/2}+2(x_{rw}x_{rr})^{1/2}+2(x_0x_{rr})^{1/2}+x_{rr}+x_{rw}]\\&+x_w[2(x_0x_{rw})^{1/2}+2(x_{rw}x_{ww})^{1/2}+2(x_0x_{ww})^{1/2}+x_{ww}+x_{rw}]\\&+4(x_0x_rx_wx_{rw})^{1/2}+2(x_0x_rx_wx_{rr})^{1/2}+2(x_0x_rx_wx_{ww})^{1/2}\\&+2(x_rx_wx_{rw}x_{ww})^{1/2}+2(x_rx_wx_{rw}x_{rr})^{1/2}+2(x_rx_wx_{rr}x_{ww})^{1/2}\}\,,\end{aligned} \tag{3.26a}$$

$$V/2NK=(\epsilon_1/K)(x_r+x_w)+(\epsilon_2/K)x_0-\tfrac{1}{2}(\lambda/K)(x_{rr}+x_{ww})-(J/K)(1-2x)^2\,, \tag{3.26b}$$

where for notational convenience $\bar{x}_\alpha\equiv x_\alpha$. The energy is a function of four dimensionless parameters and implementation of Eqs. (3.24) leads to a set of five coupled algebraic equations. These represent the principal results of the present work.

A structural quantity of interest is the single proton density matrix

$$\rho(r)\equiv\langle\Psi_t\,|\,\delta(r-r_1)\,|\,\Psi_t\rangle\,, \tag{3.27}$$

which represents the probability of finding a proton at position r along the bond. For the present theory, an elementary manipulation yields the explicit result

$$\rho(r)=\tfrac{1}{2}\{[x^{1/2}+(1-x)^{1/2}]\Phi_0(r)+[x^{1/2}-(1-x)^{1/2}]\Phi_1(r)\}^2+\tfrac{1}{2}\{S-2[x(1-x)]^{1/2}\}[\Phi_0(r)+\Phi_1(r)][\Phi_0(r)-\Phi_1(r)], \tag{3.28}$$

where S is the tunneling element defined in Eq. (3.16). The functions $\Phi_0(r)$ and $\Phi_1(r)$ are the independent proton ground and first excited eigenstates, respectively, obtained by solving the corresponding Schrödinger equation for a particular choice of bond potential. It is the symmetric and antisymmetric linear combination of these functions that represent the localized proton states corresponding to $S_l^z=\pm 1$ in the two-state model. Note that even in the disordered phase ($x=\frac{1}{2}$), $\rho(r)$ is not simply the independent particle result but is modified due to short-range correlations that tend to inhibit tunneling (i.e., cause $S<1$). Other properties of interest such as the static dielectric constant and pair correlation function can also be straightforwardly computed with in the present formalism.

In summary, the fundamental quantities in our random-mixing theory are the four self-consistently determined vertex state concentrations, $\{\bar{x}_\alpha\}$, and the long-range-order parameter, $\bar{x}$. The present theory is distinguished from previous attempts to include both short- and long-range correlations by *not* involving the matrix diagonalization of finite cluster Hamiltonians. The latter approach leads to unphysical anti-Curie-type behavior at low temperatures. The present theory has avoided this catastrophe by focusing attention on the global oxygen vertex-type concentrations as order parameters. Of course, since our theory is of an order-parameter nature it predicts classical critical behavior.

IV. APPLICATION: ONE-DIMENSIONAL TRANSVERSE ISING MODEL

The one-dimensional (1D) transverse Ising model (TIM) consists of the following Hamiltonian expressed in terms of the standard Pauli matrices:

$$H=-K\sum_{l=1}^{N}S_l^x-J\sum_{l=1}^{N}S_l^zS_{l+1}^z+NJ\,, \tag{4.1}$$

where N is the number of spins (or protons) and $S_l^z=\pm 1$. For our purposes, this Hamiltonian can be thought of as arising from the model ferroelectric pictured in Fig. 2. The nearest-neighbor coupling between protons gives rise to a polarized classical ground state with all the protons residing on the same side of the bond. This long-range order is opposed by thermal fluctuations and quantum-mechanical tunneling. The model is exactly solvable[14] and at finite temperature exhibits no phase transition to an ordered state. At zero temperature, however, there is an

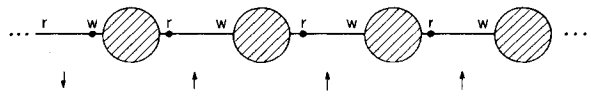

FIG. 2. Section of the one-dimensional crystal described by the transverse Ising model. The two sides of the bond are labeled right (r) and wrong (w) and correspond to $S^z=\pm 1$, respectively. An equivalent representation associates the two possible proton positions with a spin-$\frac{1}{2}$ object at the bond center.

order-disorder transition at a specific value of the parameter J/K. This feature serves as a convenient test case for gauging the accuracy of our approximate random-mixing (RM) theory, even though the underlying lattice of vertices has coordination number two, rather than four.

To analyze the 1D TIM within the framework of our theory we first observe that a full classification of the vertices requires five number operators or order parameters, N_r,N_w,N_{rw},N_0,N_x. As before N_r denotes the number of vertices with a single proton in the right position, N_{rw} denotes the number of vertices with two protons, etc. The long-range order is characterized by the total number of protons in the right position as defined by $N-N_x\equiv N(1-x)$.

To apply our RM theory we must express the potential energy term in Eq. (4.1) in terms of the relevant order parameters. It is easy to show that

$$\tfrac{1}{2}\sum_{l=1}^{N}(1+S_l^zS_{l+1}^z)=N_r+N_w\ . \tag{4.2}$$

The Hamiltonian can then be written as

$$H=-K\sum_{l=1}^{N}S_l^x+2J(N_0+N_{rw})\ , \tag{4.3}$$

where certain linear relations between the N_α's have been employed (see Appendix A). A detailed derivation of the random-mixing approximation trial ground-state energy is presented in Appendix A. The result is

$$E/N=-2K[\bar{x}(1-\bar{x})]^{-1/2}\times[\bar{x}_0(\bar{x}_r+\bar{x}_w)+2\bar{x}_0(\bar{x}_r\bar{x}_w)^{1/2}]+4J\bar{x}_0\ , \tag{4.4}$$

where $\{\bar{x}_\alpha\equiv\langle\Psi_t\,|\,N_\alpha\,|\,\Psi_t\rangle/N\}$ are variational parameters. As shown in Appendix A, there are only two independent variational parameters, which we choose to be $\bar{x}_0,\bar{x}$. Energy minimization yields two coupled algebraic equations which can be solved in closed form. Introducing the quantities

$$\bar{u}_0\equiv\tfrac{1}{2}-\bar{x}_0,\quad \bar{u}\equiv\tfrac{1}{2}-\bar{x},\quad \gamma\equiv J/K\ , \tag{4.5}$$

one can show that

$$\bar{u}_0(\gamma)=\begin{cases}(1+\frac{1}{2}\gamma)/4, & \gamma\le\gamma_c\\ g(\gamma), & \gamma\ge\gamma_c\end{cases} \tag{4.6}$$

$$\bar{u}(\gamma)=\begin{cases}0, & \gamma\le\gamma_c\\ \{g^2(\gamma)-g^{-2}(\gamma)[\frac{1}{4}-g^2(\gamma)]^2\}^{1/2}, & \gamma\ge\gamma_c\end{cases} \tag{4.7}$$

where $\gamma_c\equiv 2(\sqrt{2}-1)$ locates the critical transition point and $g(\gamma)$ is a soluton of

$$g(2g-\tfrac{1}{2})(\tfrac{1}{4}-g^2)+(\tfrac{1}{4}-g^2)^2+g^3(g-\tfrac{1}{2})-\frac{\gamma}{2}(\tfrac{1}{4}-g^2)^{3/2}=0\ . \tag{4.8}$$

The random-mixing theory value for the critical value, γ_c, of J/K is presented in Table I along with the exact result. For comparison purposes, the predictions of the standard mean-field theory (MFT), cumulant cluster theory,[6] and a variational renormalization-group calculation[15] are also indicated. The random-mixing theory represents a significant improvement over MFT. To put the result in a more familiar context, the random-mixing theory is a more accurate approximation for the transition point [$\gamma_c=0.828$ vs $\gamma_c(\text{exact})=1$] than the standard quasichemical Bethe pair approximation is for the *classical* two-dimensional Ising model ($\beta_cJ=0.347$ versus the exact Onsager value of 0.443). To the extent that the transition point is a reliable barometer of the quality of an approximation, we conclude that the random-mixing approach is at least as accurate as a pair theory.

To further explore the accuracy of the present theory, exact and approximate calculations of the polarization and ion concentration are presented in Figs. 3 and 4. The random-mixing result for the polarization is quite good and represents a significant improvement over MFT due to the inclusion of short-range correlations. The remaining deviation of the RM theory from the exact result is due to our neglect of long-range critical fluctuations. However, many properties of interest are of a more local nature and hence are not as sensitive to the long-range correlations. The ion concentration is such a property and as seen from Fig. 4 the random-mixing theory is nearly exact for this quantity. Similar agreement is found for other properties such as the average kinetic energy operator, $\langle S^x\rangle$, and the ground-state energy. Deviations of the latter quantity from its exact value are typically less than 1% except in a narrow region surrounding the critical point where errors are still no larger than 2.5%.

In three dimensions one expects the importance of long-range critical fluctuations to decrease compared to the short-range correlation effects. Indeed, if the short-range proton interactions are sufficiently strong, the phase transition can become discontinuous (first order) and critical fluctuations are absent entirely. This is often the situation for many materials of experimental interest.

TABLE I. Critical value of $\gamma\equiv J/K$ for the 1D TIM.

Theory	γ_c
Exact[a]	1.000
Random mixing	0.828
Mean field	0.500
Renormalization group[b]	0.727
Cumulant cluster[c]	No transition

[a]Reference 14.
[b]Reference 15.
[c]Reference 6.

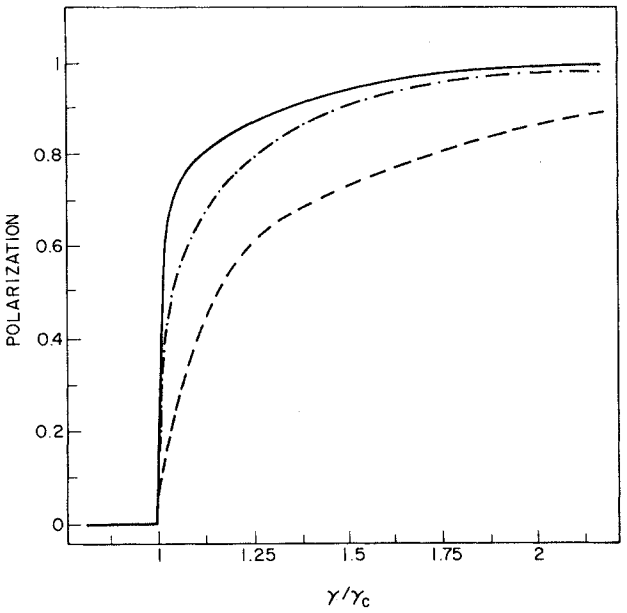

FIG. 3. Spontaneous polarization or long-range-order parameter ($|1-2x|$) for the 1D transverse Ising model plotted as a function of the scaled variable $\gamma/\gamma_c \equiv (J/K)/(J/K)_c$. The exact (solid curve), random-mixing theory (dashed-dotted curve), and mean-field-theory (dashed curve) predictions are shown.

V. MODEL CALCULATIONS

The purpose of the present section is to explore the general features predicted by the random-mixing theory for three-dimensional crystals. Application of the theory requires specification of the four dimensionless energy scales: $\epsilon_1/J, \epsilon_2/J, \lambda/J, K/J$, and numerical solution of the five coupled algebraic equations given by Eqs. (3.24)—(3.26). We proceed by considering a specific example. The parameters ϵ_1/J and ϵ_2/ϵ_1 are chosen to be 20 and 4, respectively. These values are in the range appropriate for many hydrogen-bonded ferroelectrics. The parameter λ/J is a measure of local anisotropy due to the presence of a preferred crystal axis. For a perfect tetrahedral solid like cubic ice $\lambda=0$. However, for many ferroelectrics such as the KDP family λ/J takes on values[8] in the range of 2—4. The effect of applied pressure is to increase the parameter K/J continuously. Assuming a common microscopic origin (e.g., dipolar) for the proton-proton energies $(\epsilon_1, \epsilon_2, \lambda, J)$ all the dimensionless energy scales enumerated above are pressure independent except K/J. With the above motivation, the variational equations were numerically solved and the results are displayed in Figs. 5 and 6.

The behavior of the long-range-order parameter (assumed to be proportional to the macroscopic polarization) as a function of pressure is very sensitive to the degree of local anisotropy, λ. In particular the thermodynamic nature of the transition changes from discontinuous to continuous at a value of $\lambda/J=3.79$. The sharpness of the transition is also an increasing function of ϵ_1/J. This is as expected since larger values of the latter parameter correspond to stronger short-range proton correlations. The overall trends are qualitatively similar to the predictions of the *classical* cluster theory[12,13] where temperature (playing the role of pressure) is a source of thermal (as opposed to quantum tunneling) fluctuations. Of course there are

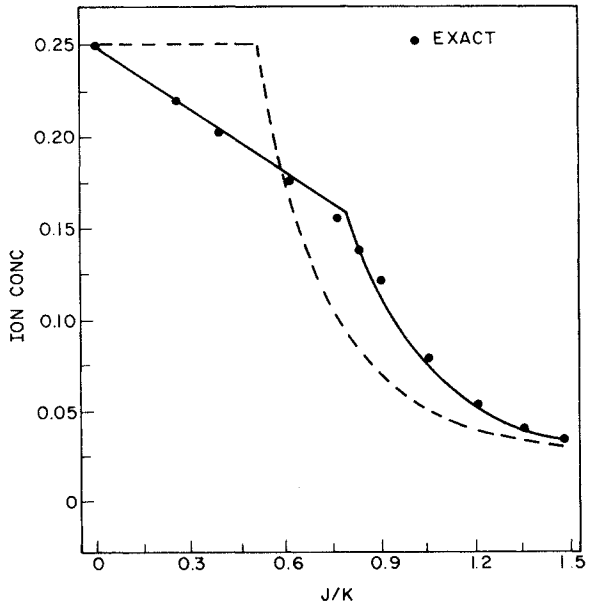

FIG. 4. Ion concentration ($\bar{x}_0=\bar{x}_{rw}$) for the 1D transverse Ising model as a function of J/K. The random-mixing-theory (solid curve) and mean-field result (dashed line) are compared with the exact values (solid circles).

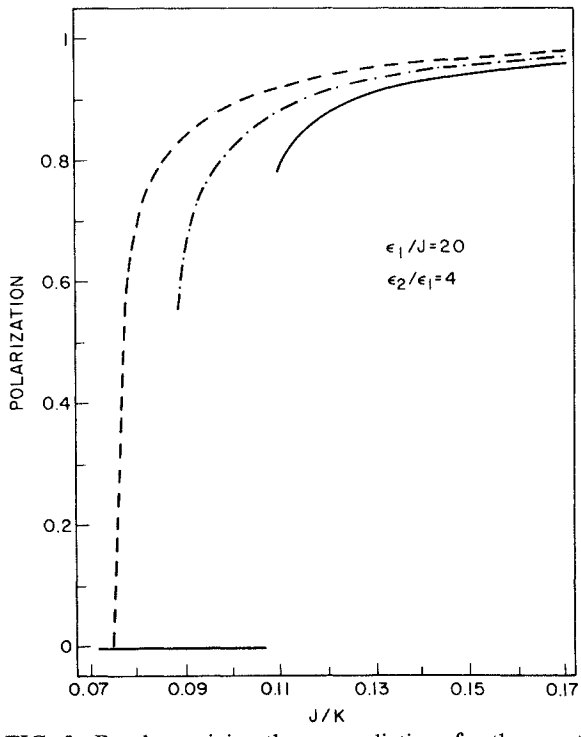

FIG. 5. Random-mixing-theory predictions for the spontaneous polarization as a function of J/K for the 3D model discussed in the text. The three curves correspond to three choices for the local anisotropy parameter: $\lambda/J=0$ (solid curve), $\lambda/J=2$ (dashed-dotted curve), and $\lambda/J=4$ (dashed curve).

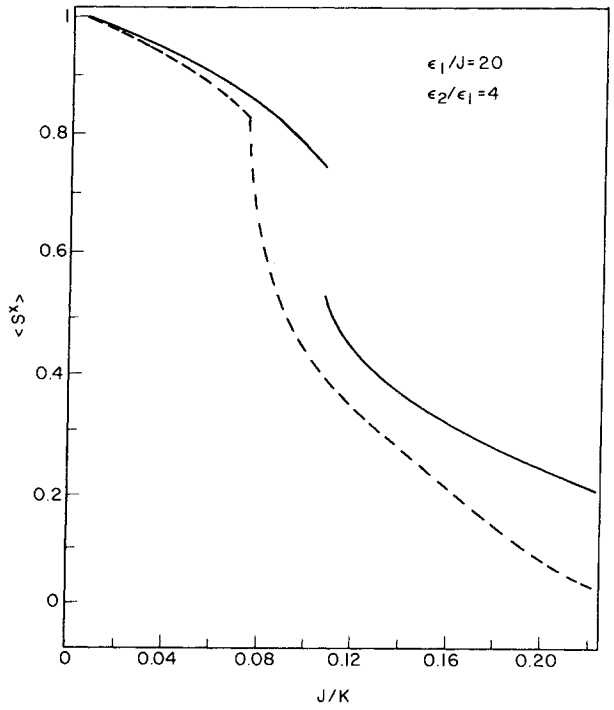

FIG. 6. Random-mixing-theory predictions for the kinetic energy matrix element as a function of J/K for the 3D model discussed in the text. The two curves correspond to $\lambda/J=0$ (solid curve) and $\lambda/J=4$ (dashed curve).

fundamental differences between the two fluctuation mechanisms since the thermal effects are activated (i.e., contribute in a Boltzmann factor fashion) while quantum tunneling induces fluctuations via state mixing.

At the transition the contribution of ionic configurations is very large. For the $\lambda=0$ case the fraction of vertices that are singly "charged" ions (vertices surrounded by one or three protons) is 0.12. This is significantly less then the purely random statistical value of 0.25, but indicates that the transition is driven by the appearance of a large number of ions in the crystal.

Another property of some interest is the kinetic energy or tunnel matrix element, $\langle S^x \rangle$. At zero temperature, if protons moved independently in their respective bonds then $\langle S^x \rangle$ would be unity. However, short- and long-range proton-proton interactions in the condensed phase will tend to oppose quantum tunneling and reduce $\langle S^x \rangle$. The amount of reduction can be taken as a measure of the effective tunnel splitting in the crystal via the relation

$$K_{\text{eff}} \equiv K \langle S^x \rangle \ . \tag{5.1}$$

The pressure dependence of this quantity is shown in Fig. 6. For the case of a discontinuous phase transition, $\langle S^x \rangle$ itself exhibits a jump discontinuity. In terms of the real-space proton position this implies a discontinuous expansion of the proton charge density, $\rho(r)$, upon going from the ordered to disordered phase. It is also interesting to note that even in the disordered phase proton tunneling is significantly inhibited due to short-range proton correlations.

Other properties such as the static dielectric constant and pair correlation function can also be computed. Structural questions such as hydrogen-bond symmetrization are also amenable to our theoretical analysis. For many hydrogen-bonded materials the oxygen-oxygen separations are sufficiently short ($\sim$2.5 Å) that modest pressures ($\sim$20 kbar) can affect significant deformations of the proton bond potential. This has allowed experimental study of many of the pressure-induced phenomena of concern in this paper. Detailed application of the present theory to measurements on hydrogen-bonded ferroelectric crystals will be presented in a planned future publication.[10]

VI. DISCUSSION

We have developed a ground-state correlated wave-function theory for the equilibrium properties of hydrogen-bonded crystals. To the best of our knowledge, it represents the first internally consistent theory that simultaneously incorporates short- and long-range proton correlations and two-state quantum-mechanical tunneling. The predictions of the theory for the exactly solvable one-dimensional quantum Ising model in conjunction with general statistical mechanical considerations suggest that it is a quantitatively reliable theory for a range of experimentally relevant three-dimensional crystals. Consequently, the theory should be a useful tool for predicting and interpretating high-pressure-induced phenomena in hydrogen-bonded materials at low temperature. In particular, for the well-studied KDF-like ferroelectrics, the theory is directly applicable[10] to the interpretation of measurements[2,16,17] of the pressure dependence of the static dielectric constant and macroscopic polarization, and their variability upon isotope substitution. Material specific parameters can be extracted by fitting the theory to the high-pressure experimental data, thereby providing microscopic information complementary to the usual low-pressure variable temperature studies.[8]

Another application is to the high-pressure behavior of ice polymorphs.[9] For these crystals, the ion formation energies are much larger than for KDP-like ferroelectrics. Consequently, significantly higher pressures ($\approx$500 kbar) are expected to be required to observe phenomena such as order-disorder phase transitions and hydrogen-bond symmetrization. Therefore, the availability of a quantitatively reliable theory to guide the difficult very-high-pressure experiments is even more crucial for these systems.

Many avenues of future research remain to be considered. The effect of lattice vibrations (phonons), isotopic (H and D) mixtures, and a description beyond the two-state level are a few of the obvious generalizations that can be pursued. Perhaps the most urgent need is the generalization of the theory to finite temperatures. Such a task should be possible by employing the finite temperature analog of the physical content of the random-mixing approximation. On a qualitative level, one expects the one-dimensional character of proton motions in the linear hydrogen bonds will rule out the existence of low-lying excited states of a spin-wave nature as is found for the three-dimensional Heisenberg magnet. One possibility is a particlelike excitation spectrum possessing a finite gap be-

tween the ground and first excited states. In this case, the ground-state theory developed in the present paper would be applicable when the thermal energy is small compared to the energy gap. On a quantitative level, the fundamental object at nonzero temperature is the diagonal density matrix or thermal propagator. Present research is geared to deriving a closed equation of motion for this object in terms of a finite set of order parameters which are subsequently determined by free-energy minimization. We hope to report on this work in a future publication.

APPENDIX A

We consider in detail the calculation of the kinetic energy matrix element for the one-dimensional transverse Ising model discussed in Sec. IV. A full classification of the vertices employs the five number or order parameters: $N_r, N_w, N_{rw}, N_0, N_x$. Particle conservation, charge neutrality, and long-range-order parameter definition lead to the relations

$$\begin{aligned} &N_{rw}+N_r+N_w+N_0=N\ , \\ &N_{rw}-N_0=0\ , \\ &N_{rw}+N_w=N_x\equiv Nx\ . \end{aligned} \tag{A1}$$

These equations allow one to reduce the vertex classification to two independent parameters. Choosing N_0 and N_x as independent, the remaining three concentrations or mole fractions are given by

$$\begin{aligned} &x_{rw}=x_0\ , \\ &x_r=1-x-x_0\ , \\ &x_w=x-x_0\ , \end{aligned} \tag{A2}$$

where $x_\alpha\equiv N_\alpha/N$.

For a tagged bond, there are $2\times4=8$ possible bond configurations. These naturally break up into two groups corresponding to the tagged proton being on the right or wrong side of the bond. The eight possibilities are listed in Table II. The probability that the proton in the tagged bond is in the right (wrong) position with the connected vertices of type (μ,ν) is denoted by $p^{(r)}(\mu\mid\nu)$ $[p^{(w)}(\mu\mid\nu)]$. Within the context of the random-mixing approximation for the configuration $\{x_\alpha\}$ this is given by

$$p^{(\alpha)}(\mu\mid\nu)\equiv C^{(\alpha)}x_\mu x_\nu g^{(\alpha)}(\mu\mid\nu),\quad \alpha=r,w \tag{A3}$$

where $C^{(\alpha)}$ is a normalization factor determined by the sum rules

$$\begin{aligned} &\sum_{\mu,\nu}p^{(r)}(\mu\mid\nu)\equiv1-x\ , \\ &\sum_{\mu,\nu}p^{(w)}(\mu\mid\nu)\equiv x\ , \end{aligned} \tag{A4}$$

and $g^{(\alpha)}(\mu\mid\nu)$ is a compatibility factor which in the present case is either 1 or 0 depending on whether the configuration (μ,ν) is allowed or not allowed. For example, $g^{(r)}(rw\mid rw)=g^{(w)}(rw\mid rw)=0$, while $g^{(r)}(rw\mid r)=g^{(w)}(w\mid rw)=1$. For the present problem there are $2\times4^2=32$ distinct $g^{(\alpha)}(\mu\mid\nu)$'s. Simple considerations reveal that only eight are nonzero. This result combined with Eqs. (A3) and (A4) lead to the probabilities shown in Table II.

TABLE II. Bond configurations and their probabilities. The symbols r and w refer to the cases when the proton is on the right and wrong side of the bond, respectively.

r		w	
Probability	Vertex state	Vertex state	Probability
$x_rx_{rw}(1-x)^{-1}$	(rw,r)	(w,rw)	$x_wx_{rw}x^{-1}$
$x_0x_{rw}(1-x)^{-1}$	$(rw,0)$	(w,w)	$x_w^2x^{-1}$
$x_r^2(1-x)^{-1}$	(r,r)	$(0,rw)$	$x_0x_{rw}x^{-1}$
$x_rx_0(1-x)^{-1}$	$(r,0)$	$(0,w)$	$x_0x_wx^{-1}$

The calculation of the kinetic energy matrix element proceeds by employing the results of Table II in conjunction with the formula given in Eq. (3.19). Recalling that we have chosen N_0 and N_x as the independent variables one obtains

$$\langle\Psi\mid T\mid\Psi\rangle\equiv-KNS\ , \tag{A5}$$

$$\begin{aligned} S=\sum_{\{N_0,N_x\}}\Omega(N_0,N_x)A(N_0,N_x)[&2x_rx_0(1-x)^{-1}A(N_0,N_x+1)+x_0^2(1-x)^{-1}A(N_0-1,N_x+1) \\ &+x_r^2(1-x)^{-1}A(N_0+1,N_x+1)+2x_0x_wx^{-1}A(N_0,N_x-1) \\ &+x_w^2x^{-1}A(N_0+1,N_x-1)+x_0^2x^{-1}A(N_0-1,N_x-1)]\ . \end{aligned} \tag{A6}$$

Further simplification is effected by employing Eq. (3.22). For the 1D TIM we have

$$\Omega(N_0,N_x)=\frac{N!}{N_r!N_w!N_{rw}!N_0!}\left(\tfrac{1}{4}\right)^{N_r+N_w+N_{rw}+N_0} \times x^{Nx}(1-x)^{N(1-x)} \tag{A7}$$

and hence

$$\frac{A(N_0+n_0,N_x+n_x)}{A(N_0,N_x)}=\left[\frac{1-x}{x}\right]^{n_x/2} \times x_0^{n_0}x_w^{(n_x-n_0)/2}x_r^{-(n_0+n_x)/2}\ , \tag{A8}$$

where n_0,n_x can assume the values $0,\pm1$. Combining Eqs. (A6) and (A8) yields

$$S=\sum_{\{N_0,N_x\}}\Omega(N_0,N_x)A^2(N_0,N_x)2[x(1-x)]^{-1/2}\times[2x_0(x_rx_w)^{1/2}+x_0(x_r+x_w)]$$

$$=2[\bar{x}(1-\bar{x})]^{-1/2}[2\bar{x}_0(\bar{x}_r\bar{x}_w)^{1/2}+\bar{x}_0(\bar{x}_r+\bar{x}_w)]\ . \quad \text{(A9)}$$

This result corresponds to the first term in Eq. (4.4) of the text. Equation (3.26b) is derived in an analogous fashion but the analysis is considerably more tedious.

APPENDIX B

An alternative approach to deriving the variational ground-state energy within the random-mixing approximation is based on the concept of a "bond orbital." This object describes the position (r or w) of a tagged proton in a particular bond and also the state of the two associated vertices. These considerations constitute a complete description of the state of a bond and suggests the introduction of bond orbitals (in ket notation): $|n_\alpha^{(\sigma)}(1)n_\gamma^{(1-\sigma)}(2)\rangle_l$. The superscript $\sigma=r,w$ (and $1-\sigma\equiv w,r$, respectively) denotes the position of the proton in the bond l, and $n_\alpha(1)$ and $n_\gamma(2)$ specifies the corresponding vertex types. The bond orbital states are formally defined by the effect of the Hamiltonian operators on them. For example, the potential-energy operator, $\epsilon_\nu N_\nu$ can be expressed as a lattice sum over vertices

$$\epsilon_\nu\hat{N}_\nu=\tfrac{1}{2}\epsilon_\nu\sum_{\theta=r,w}\sum_{i=1}^{N}\hat{n}_\nu^{(\theta)}(i)\ . \quad \text{(B1)}$$

Then

$$\hat{n}_\nu^{(\theta)}(1)\,|\,n_\alpha^{(\sigma)}(1)n_\gamma^{(1-\sigma)}(2)\rangle=\delta_{\alpha\nu}\delta_{\sigma\theta}\,|\,n_\alpha^{(\sigma)}(1)n_\gamma^{(1-\alpha)}(2)\rangle \quad \text{(B2)}$$

and

$$\langle n_\alpha^{(\sigma)}(1)n_\gamma^{(1-\sigma)}(2)\,|\,n_\beta^{(\lambda)}(1)n_\rho^{(1-\lambda)}(2)\rangle\equiv\delta_{\alpha\beta}\delta_{\gamma\rho}\delta_{\lambda\sigma}\ . \quad \text{(B3)}$$

The above relations make it clear that the bond orbitals are in an occupation number representation and the $\hat{n}_\nu^{(\theta)}(l)$ simply test whether the lth vertex is of the νth type with the associated proton in the θth position.

The effect of the kinetic energy operator for the lth proton (bond), $\hat{S}_l^x$, is to simply flip the proton to the opposite side of the bond. It does not change the positions of the secondary protons that serve to define the state of the two vertices associated with the lth bond. Of course, the hopping of the single proton in the lth bond will change the state of the corresponding two vertices in a unique fashion. With these rules, the trial ground-state wave function can be written as a product of "molecular" orbits for each bond

$$\Psi_0=\prod_{l=1}^{2N}\Phi_g(l)\ , \quad \text{(B4)}$$

where

$$\Phi_g(l)\equiv\sum_{\sigma=r,w}\sum_{\alpha,\gamma}[C^{(\sigma)}\bar{x}_\alpha\bar{x}_\gamma g^{(\alpha)}(\alpha\,|\,\gamma)]^{1/2}\times|\,n_\alpha^{(\sigma)}(1)n_\gamma^{(1-\sigma)}(2)\rangle_l\ . \quad \text{(B5)}$$

The molecular orbital, Φ_g, is a symmetric linear combination of all the possible bond orbitals with each individual coefficient given by the square root of the probability of finding the bond in a particular state as computed within the framework of the random-mixing approximation. Calculation of the energy expectation value for the trial state of Eq. (B4) yields the same result as obtained by the procedure discussed in Sec. III and Appendix A. Therefore, the alternative formulation described above provides a somewhat simpler (both conceptually and computationally) picture of the physical content of the random-mixing approximation. The role of the average values of the order parameters, $\{\bar{x}_\alpha\}$, as variational parameters is particularly clear from Eq. (B5).

[1]L. Pauling, J. Am. Chem. Soc. 57, 2680 (1935); J. D. Bernal and R. H. Fowler, J. Chem. Phys. 1, 515 (1933).

[2]For a recent comprehensive textbook discussion, see M. E. Lines and A. M. Glass, *Principles and Applications of Ferroelectrics and Related Materials* (Clarendon, Oxford, 1977).

[3]G. C. Pimentel and A. L. McClellan, *The Hydrogen Bond* (Freeman, San Francisco, 1960), p. 259.

[4]J. O. Lundgren and I. Olovsson, in *The Hydrogen Bond. II. Structure and Spectroscopy,* edited by P. Schuster, G. Zundel, and C. Sandorfy (North-Holland, New York, 1976), p. 497.

[5]F. H. Stillinger and K. S. Schweizer, J. Phys. Chem. 87, 4281 (1983).

[6]R. Blinc and S. Svetina, Phys. Rev. 147, 423 (1966); 147, 430 (1966).

[7]V. G. Vaks and V. I. Zinenko, Zh. Eksp. Teor. Fiz. 64, 650 (1973) [Sov. Phys.—JETP] 37, 330 (1973)].

[8]V. G. Vaks, N. E. Zein, and B. A. Strokov, Phys. Status Solidi 30, 801 (1975).

[9]K. S. Schweizer and F. H. Stillinger, J. Chem. Phys. (to be published).

[10]K. S. Schweizer and F. H. Stillinger (unpublished).

[11]J. C. Slater, J. Chem. Phys. 9, 16 (1941).

[12]Y. Takagi, J. Phys. Soc. Jpn 3, 271 (1948).

[13]M. E. Senko, Phys. Rev. 121, 1599 (1961).

[14]P. Pfeuty, Ann. Phys. (N.Y.) 57, 79 (1970).

[15]S. D. Drell, M. Weinstein, and S. Yankielowicz, Phys. Rev. D 16, 1769 (1977).

[16]G. A. Samara, Phys. Rev. Lett. 27, 103 (1971); Ferroelectrics 5, 25 (1973); 7, 221 (1974).

[17]P. S. Peercy and G. A. Samara, Phys. Rev. B 8, 2033 (1973).